

Thermal properties of structurally balanced systems on classical random graphs

Krzysztof Malarz* and Maciej Wołoszyn†

AGH University of Science and Technology, Faculty of Physics and Applied Computer Science, al. Mickiewicza 30, 30-059 Kraków, Poland

(Dated: June 30, 2022)

The dynamics of social relations and the possibility of reaching the state of structural balance (Heider balance) under the influence of the temperature modeling the social noise level are discussed for interacting actors occupying nodes of classical random graphs. Depending on the graph density D , either a smooth cross-over or a first-order phase transition from a balanced to an imbalanced state of the system is observed with an increase of the thermal noise level. The minimal graph density D_{\min} for which the first-order phase transition can be observed decreases with system size N as $D_{\min} \propto N^{-0.58(1)}$. For graph densities $D > D_{\min}$ the reduced critical temperature $T_c^* = T_c/T_c(D=1)$ increases with the graph density as $T_c^* \propto D^{1.719(6)}$ independently of the system size N .

I. INTRODUCTION

The signed network with positive and negative link values $x_{ij} = \pm 1$ representing friendly and hostile relations among actors—occupying network nodes i and j —is termed structurally balanced [1] when in every triangle these relations obey Heider's rules [2]:

- a friend of my friend is my friend,
- a friend of my enemy is my enemy,
- an enemy of my friend is my enemy,
- an enemy of my enemy is my friend.

The triangles where these rules are not violated are termed balanced (in the Heider sense). The appearance of (imbalanced) triangles that do not obey these rules leads to the appearance of mental stress known as cognitive dissonance [3]. Four possible signed triangles are shown in Figure 1. Among them, those with the sum $s = x_{ij} + x_{jk} + x_{ki}$ equal to +3 and -1 are balanced, while two others are not and i, j, k are the labels of the triangle vertices.

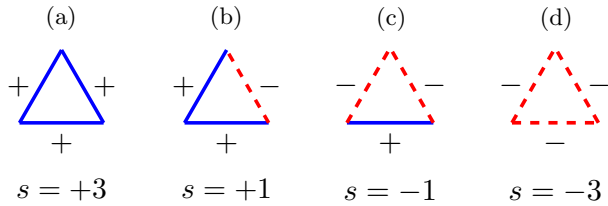


FIG. 1: (Color online). Heider's triads corresponding to balanced [(a) and (c)] and imbalanced [(b) and (d)] states. Solid blue lines and dashed red lines represent friendly (positive, $x_{ij} = +1$) and hostile (negative, $x_{ij} = -1$) relations, respectively. The values of $s = x_{ij} + x_{jk} + x_{ki}$ are presented in the bottom of subfigures and i, j, k are the triangles vertices labels.

Several techniques are applied for modeling the resolving of the stress mentioned above, in which the imbalanced triangles are subsequently eliminated, leading the system towards the Heider balance (see Ref. 4 for review). For example, with the cellular automaton technique [5] and the triangular lattice, the deterministic rule

$$x_{ij}(t+1) = \text{sign}(x_{im}(t)x_{jm}(t) + x_{in}(t)x_{jn}(t)) \quad (1)$$

is applied synchronously to all links x_{ij} (where i, j, m , and n are node labels in a pair of triangles ijm and ijn having a common edge ij). For a complete graph [6], the rule (1) may be generalized as

$$x_{ij}(t+1) = \text{sign}\left(\sum_k x_{ik}(t)x_{jk}(t)\right), \quad (2)$$

where $k \neq i, j$ is the node label of the third vertex of the triangle. Finally, Equation (2) can be further generalized to any network [7] defined by its adjacency matrix $\mathbf{A} = [a_{ij}]$ as

$$x_{ij}(t+1) = \text{sign}\left(\sum_k a_{ik}x_{ik}(t) \cdot a_{jk}x_{jk}(t)\right), \quad (3)$$

for existing edges (where $a_{ij} = 1$). The (binary and symmetric) adjacency matrix $\mathbf{A} = [a_{ij}]$ elements

$$a_{ij} = \begin{cases} 1 & \iff i \text{ and } j \text{ are connected,} \\ 0 & \iff \text{otherwise,} \end{cases} \quad (4)$$

define the network. In all cases [Equations (1) to (3)] if the argument for the function $\text{sign}(\dots)$ is zero, x_{ij} remains unchanged.

The time evolution of the system may also be governed by a set of differential equations [8–14]

$$\dot{x}_{ij} = \sum_k x_{ik}x_{jk}, \quad (5)$$

where x_{ij} denotes the (real) value on the edge between the nodes i and j and the summation passes through all

* 0000-0001-9980-0363; malarz@agh.edu.pl

† 0000-0001-9896-1018; woloszyn@agh.edu.pl

the nodes k that make up the triangles ijk . This equation is solvable analytically; however, x_{ij} tends to infinity in a finite time [12]. To evade this problem, the solution is either to impose numerically the condition that $|x_{ij}| < 1$, or to use the expression $(1 - x_{ij}^2)$ as a prefactor [13]. With this modification, Equation (5) generically drives the system to one of 2^{N-1} balanced states. Other stationary solutions (the so-called jammed states) are also possible [14], similarly to the discrete evolution [15].

For modeling the level of social noise (equivalent to the non-zero temperature [16]), the deterministic rules [Equations (1) to (3) and (5)] should be replaced by the probabilistic ones. Examples of such rules (governed by the heat-bath algorithm [17, 18]) were applied to the linear chain of actors [19], the triangular lattice [20], diluted and densified triangulations [7] and complete graphs [21–24]. In the latter case, approximated mean-field solutions are also available [21, 25, 26]. In the presence of thermal noise, the system undergoes a phase transition from a balanced (low noise level) to an imbalanced (high noise level) state.

Recently, the absence of the above-mentioned phase transition was observed for the triangular lattice [20]: independently on the noise level, the system remains in an imbalanced phase. However, signatures of various types of phase transitions were also described in earlier works on structurally balanced systems [19, 27].

Intrigued by those observations, we checked the thermal evolution of the system for diluted and enriched triangular lattices [7]. We found that both the balanced (or partially balanced) and imbalanced states are possible if the average node degree is far enough from that of the regular triangular lattice. The former state is observed at lower temperatures (noise levels) and the latter at higher temperatures. Diluted triangular lattices and less enhanced networks show a smooth cross-over between those two states, and a phase transition of the first kind is observed for graphs of sufficiently high density. In enhanced triangular lattices, the temperatures of the crossover as well as critical temperatures of the phase transition depend on the system size, whereas the crossover temperatures in diluted triangular lattices are size-independent. If lattices are created by adding or removing only a small fraction of links to or from the regular triangular lattice, balanced states are not possible.

In this paper, we take a step further in investigating this issue and check the influence of thermal noise on structural balance in classic random graphs [28–31].

II. MODEL

When the evolution of the system is governed by the heat-bath algorithm [17, 18], [32, p. 154] the deterministic rules [Equations (1) to (3) and (5)] should be replaced

by the probabilistic ones,

$$x_{ij}(t+1) = \begin{cases} +1 & \text{with probability } p_{ij}(t), \\ -1 & \text{with probability } [1 - p_{ij}(t)], \end{cases} \quad (6a)$$

where

$$p_{ij}(t) = \frac{\exp[\xi_{ij}(t)/T]}{\exp[\xi_{ij}(t)/T] + \exp[-\xi_{ij}(t)/T]}. \quad (6b)$$

T is the temperature (noise level) at which the evolution occurs and

$$\xi_{ij}(t) = \sum_k a_{ik}x_{ik}(t) \cdot a_{kj}x_{kj}(t). \quad (6c)$$

Classical random graphs can be formed by a random combination of N nodes with L edges (the Erdős–Rényi construction [28, 29]), or by implementing each of the possible $N(N-1)/2$ connections between nodes with a specified probability D (the Gilbert construction [33]). In the thermodynamic limit ($N \rightarrow \infty$) both, the Gilbert and Erdős–Rényi constructions lead to the same result ($D = 2L/[N(N-1)]$) [34]. Here, we apply the Gilbert approach and term the probability D as a *graph density*. Then, every element of the adjacency matrix $a_{ij} = a_{ji}$ ($i \neq j$) is set to 1 with probability D or 0 with probability $(1-D)$.

The Heider balance can be easily identified by checking the system work function [15, 35]

$$U \equiv -\frac{\text{Tr}[(\mathbf{A} \circ \mathbf{X})^3]}{\text{Tr}(\mathbf{A}^3)}, \quad (7)$$

where \circ stands for the Hadamard product of matrices and matrix $\mathbf{X} = [x_{ij}]$. The system work function U is equal to -1 if and only if all triangles in the system are balanced.

Finally, to check the presence and kind of phase transition, we use the fourth-order Binder cumulant K [32, p. 78] of the work function U defined as

$$K \equiv 1 - \frac{\langle U^4 \rangle}{3\langle U^2 \rangle^2}, \quad (8)$$

where $\langle \dots \rangle$ denotes averaging over independent simulations.

The type of the phase transition can be determined for a particular network based on the details of Binder cumulant dependence on temperature:

- the first order (abrupt) phase transition is indicated by a deep minimum of $K(T)$, which is observed in the vicinity of the critical temperature T_c [32, p. 85], [36, 37],
- the second order (continuous) phase transition corresponds to K changing smoothly from $K = 2/3$ at low temperatures to $K = 0$ at high temperatures [37], [38, p. 508] with non-trivial behavior of $K(T_c)$ for various system sizes [32, p. 80].

III. RESULTS

Our simulations performed on classical random graphs cover the whole range of graph densities D for which the possibility of structural balance can be analyzed. We start from values of density close to zero (at least one triad is needed) and proceed to $D = 1$ (which is simply the complete graph), considering system sizes varying between $N = 50$ and $N = 400$. In all cases, the initial state is imbalanced ($U = 0$), with each x_{ij} randomly set to -1 or $+1$ with the same probability. All results presented below were obtained by completing the $t_{\max} = 10^4$ time steps, of which the last $\tau = 10^3$ were taken into account during the averaging procedure to find the outcome of a simulation. For each set of parameters (temperature T , graph density D , system size N) $R = 100$ independent simulations were performed and the mean values of the required quantities were calculated.

The work function given by Equation (8), which allows us to distinguish between balanced and imbalanced states, is calculated against the temperature. Figure 2 shows the results of the calculations performed for several different densities, from relatively low $D = 0.05$ to $D = 0.5$. As expected, in the high temperature limit the system is in an imbalanced ($\langle U \rangle = 0$) and disordered ($\{x_{ij}\} = 0$, where $\{\dots\}$ stands for averaging over all links) state. On the other hand, in the opposite limit of $T \rightarrow 0$ the work function assumes values equal to or close to -1 , which shows that at low temperatures the system reaches a balanced state or at least becomes partially balanced. However, the change between the high- and low-temperature limits of $\langle U \rangle$ does not always occur exactly the same way. At higher graph densities, the decrease in temperature causes the work function to abruptly change from 0 to -1 at a certain temperature, whereas lower densities result in a smooth crossover from an imbalanced state toward the balanced state (not necessarily reaching the perfect balance). Comparison of parts (a), (b) and (c) of Figure 2 also indicates that the size N of the system plays a significant role, since for the same D the characteristics of $\langle U(T) \rangle$ are different for various N . In particular, the temperature at which the system becomes balanced is not the same. For a complete graph ($D = 1$) this dependence becomes $T_c \propto \sqrt{N}$ [23].

Furthermore, a more detailed study reveals that in some cases, a drop in $\langle U(T) \rangle$ resulting from the decrease in T is followed by a slight increase observed at the lowest T . This effect is clearly visible for $N = 200$ and $D = 0.15$ shown in Figure 2(b), where $\langle U \rangle \approx -1$ directly below $T_c \approx 1$, but when T is even lower the work function increases to $\langle U \rangle \approx -0.8$ when $T \rightarrow 0$. The same applies, e.g., to the case of $N = 100$ and $D = 0.25$ shown in Figure 2(a), or $N = 400$ and $D = 0.1$ shown in Figure 2(c), although in those two situations the increase of $\langle U \rangle$ when T approaches zero is much smaller.

The rapid changes observed in $\langle U(T) \rangle$ may suggest the possibility of a phase transition. To find out if this is

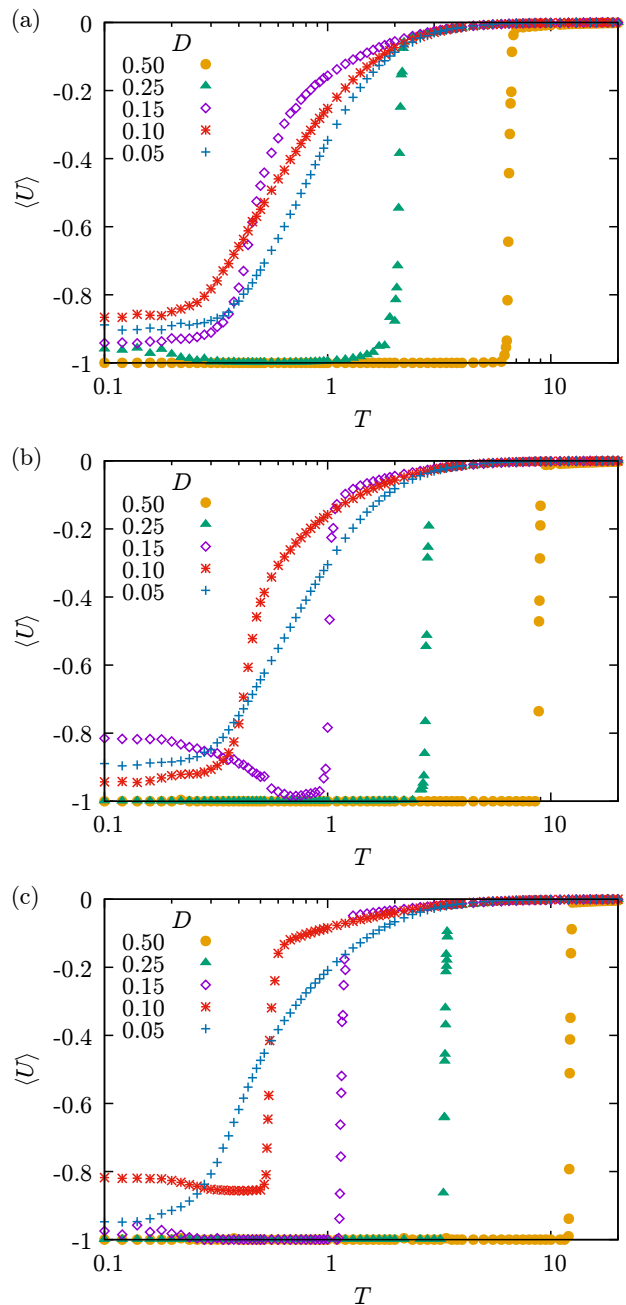


FIG. 2: (Color online). Thermal evolution of work function $\langle U \rangle$ for systems described by classical random graphs with various density D and sizes (a) $N = 100$, (b) $N = 200$, (c) $N = 400$.

actually the case, we use the fourth-order Binder cumulant K defined in Equation (8). Since we already know that the temperature at which the change occurs depends on the density of the graph, we need to find K as a function of both T and D . The result obtained for $N = 200$ is presented in Figure 3. It shows a distinct narrow minimum of K , which indicates the first-order phase transition [32, 36, 37] and can be used to determine the

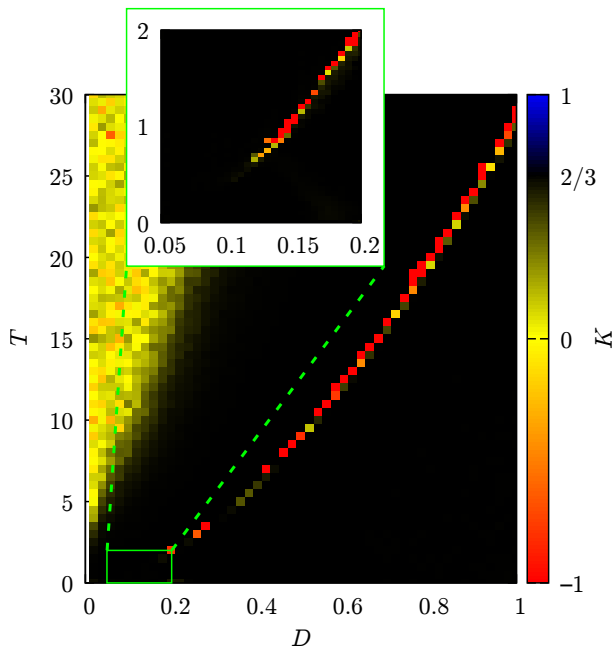


FIG. 3: The fourth-order Binder cumulant K as a function of graph density D and temperature T for $N = 200$.

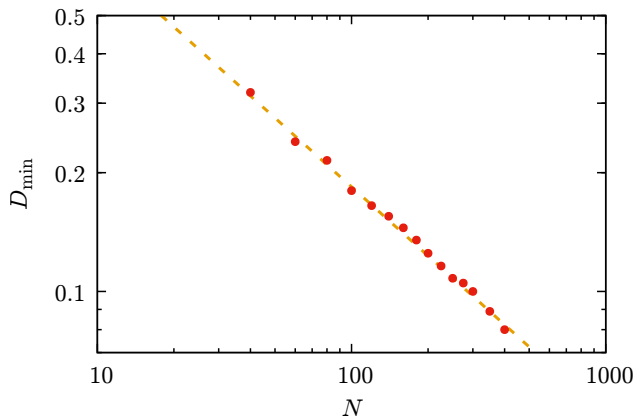


FIG. 4: The minimal density D_{\min} required for the phase transition between the balanced and imbalanced state. The dashed line is the result of least-squares fitting, $D_{\min} = 2.7(1) \cdot N^{-0.58(1)}$.

critical temperature as a function of D . However, for $N = 200$ such a minimum of K is observed only for densities greater than $D_{\min} \approx 0.12$ (see the inset of Figure 3 using a finer mesh for calculations at low D and T). Simulations performed for different system sizes reveal that the minimum density required to observe the phase transition varies exponentially with N as $D_{\min} \propto N^{-0.58(1)}$, as demonstrated in Figure 4. The data points presented in that figure were obtained from the arbitrarily chosen condition that the Binder cumulant K becomes negative.

The values of D_{\min} are also the leftmost points of

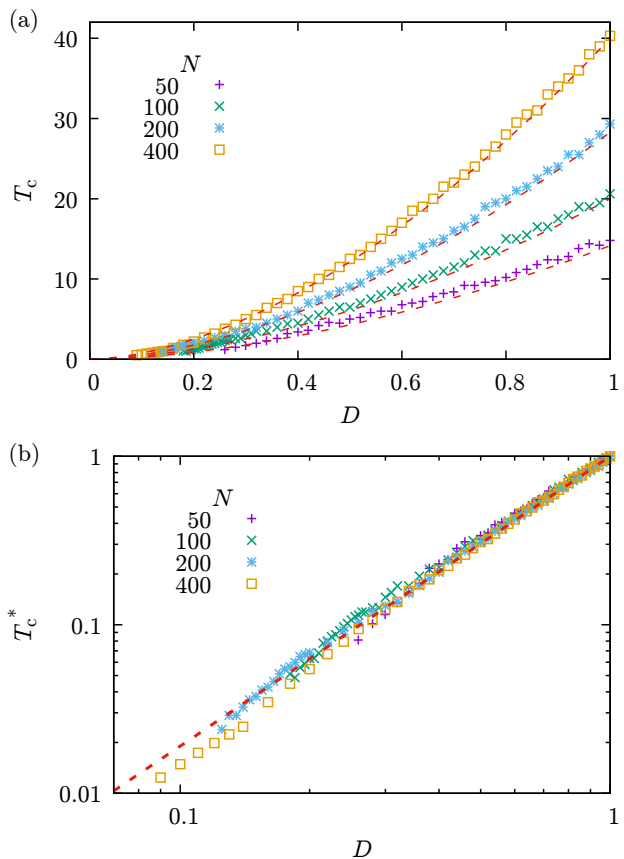


FIG. 5: (a) Critical temperature T_c found from the minimum of the fourth-order Binder cumulant K for $N = 50, 100, 200$ and 400 . Dashed line used for $2\sqrt{N}D^{1.719(6)}$. (b) Reduced critical temperature $T_c^* = T_c/T_c(D = 1)$ for the same system sizes, with dashed line showing the least-squares fitted $T_c^* = D^{1.719(6)}$.

each of the data series (corresponding to various sizes $N = 50, 100, 200$ and 400) presented in Figure 5(a). It shows the critical temperatures T_c that separate the balanced and imbalanced phases, determined as the minima of $K(T)$ for consecutive values of density D . The data in Figure 5(a) indicate that for all analyzed system sizes T_c increases with the graph density D . Furthermore, for any given D , the value of T_c increases with the size of the system. The values of $T_c(D \rightarrow 1) \propto \sqrt{N}$ approach critical temperatures already known numerically for complete graphs [23, Equation (2), Figure 2(b)]. Our results indicate that this \sqrt{N} -proportionality is preserved throughout the entire range of densities D , as shown by the dashed lines in Figure 5(a). To establish a universal size-independent relation normalized to the value at density $D = 1$, the reduced critical temperature defined as $T_c^* = T_c/T_c(D = 1)$ is calculated. Figure 5(b) shows that this reduced critical temperature increases with the graph density as $T_c^* = D^\gamma$, with $\gamma = 1.719(6)$ found using the least-squares linear fit for data in logarithmic scale.

IV. DISCUSSION

The observation that the critical temperature increases with the graph density D , but the phase transition occurs only if $D > D_{\min}$, suggests that the internal structure of the system, i.e. the properties of the graph varying with D may be related to the possibility of the phase transition. Since the dynamics in the considered model is based on the relations in triads, it is important to note that at low densities relatively few triads exist in the graph. This means that they tend to be separated with regard to the possible mutual influence on their states, which occurs only if the triads include a common relation. The lack of interaction between at least some of the triads in the system can be analyzed in terms of the number of clusters of interacting triads.

To find out how the value of D_{\min} may be related to the internal structure of the system, the number Q of non-interacting triad clusters was calculated using a version of the Hoshen–Kopelman algorithm [32, pp. 59–60], [39] adapted to the situation when neighboring triads are defined as those that have a common link. The results obtained as a function of system size N and density D are presented in Figure 6. For a given N , the two limiting cases of low and high D are self-evident. At the lowest densities, there is only a very limited number of isolated triads, each of them constituting its own cluster of one element, and hence the resulting low Q . The increase in D adds more and more triads to the system, but initially with a low probability of containing a relation that also belongs to another triad. As a result, the number of non-interacting triad clusters quickly increases. Then, when high densities are reached, the number of triads becomes very large, $\Delta = \Delta_{\text{CG}} D^3$, where $\Delta_{\text{CG}} = \binom{N}{3}$ is the number of triads in a complete graph with N nodes; obviously, it quickly reduces the number of clusters to only one.

The values of D_{\min} included in Figure 6 as green dots show that the phase transition occurs only if all triads belong to a limited number of large clusters. For smaller sizes, it comes down to just one cluster with all triads, which enables the phase transition, while for the larger systems, the density must reach a value for which the number of triads is reduced to just a few. It seems to be the property of classical random graphs that the phase transition between balanced and imbalanced states is possible only if Q is a small number. However, when systems based on other types of graphs are considered, having just one cluster that contains all triads does not guarantee that the phase transition is achievable, as illustrated by the results of simulations performed on the regular triangular lattice [7].

The fact that for densities below D_{\min} the phase transition is not observed does not mean that the system remains in an imbalanced state when the temperature decreases. As shown in Figure 2(a) for $D = 0.05, 0.10$ and 0.15 ($D_{\min} \approx 0.18$ for $N = 100$) or in Figure 2(c) for $D = 0.05$ ($D_{\min} \approx 0.08$ for $N = 400$), a partially balanced state with $\langle U(T \rightarrow 0) \rangle \approx -0.9$ is reached. In this

case, the system work function gradually changes with T during a smooth crossover from the imbalanced state.

The difference between the two regimes, above and below D_{\min} , is also visible in the proportion of the triad types in the system presented for $N = 200$ in Figure 7 (at this size, the minimum density needed for the phase transition is $D_{\min} \approx 0.13$). In the first case, that is, for $D > D_{\min}$, all triads are balanced when $T < T_c$; most of them (75%) with $s = -1$, and the rest (25%) with $s = +3$. For a complete graph ($D = 1$) and a thermodynamic limit ($N \rightarrow \infty$) this ratio (75%÷25%) can be calculated based on the assumption that the system is divided into two equinumerous cliques: internally friendly triangles [$s = +3$, see Figure 1(a)] connected by hostile triangles [$s = -1$, see Figure 1(c)] [26].

When the temperature increases, these proportions change rapidly at T_c to 12.5% for each of the $s = +3$ and $s = -3$ triads, and 37.5% for each of the $s = +1$ and $s = -1$ triads, which is a simple consequence of all links x_{ij} taking random (± 1) and independent values. The second case of $D < D_{\min}$, shown in detail in Figure 7(e–h), is related to a smooth change in the proportion of triads and a lack of complete balance that manifests itself by a non-zero proportion of $s = +1$ and $s = -3$ triads even at $T \rightarrow 0$. For D just above D_{\min} , the system reaches $\langle U \rangle = -1$ for temperatures in a certain range below T_c , but quite interestingly not at the lowest temperatures. An example of such situation is discussed in Section III for the case of $D = 0.15$ and $N = 200$ [Figure 2(b)]. Figure 7(f) indicates that this situation is related to a changed proportion of triads, with approximately 10% of $s = +1$ triads (not observed in the balanced state) existing at $T \rightarrow 0$. The numbers of other types of triads are also slightly changed compared to the balanced state reached by the system at higher T , as long as the temperature is still below T_c . As a result, the region of partial balance spreads into larger densities at low T , compared to higher temperatures.

V. CONCLUSIONS

The structural balance in systems with an internal network of relations based on classical random graphs can be reached at least to some degree independently of the graph density D , provided that the level of thermal noise T is sufficiently low. It is remarkably different from the results obtained for the regular triangular lattice and its densified or diluted versions. In the presence of thermal noise even partial Heider balance is impossible not only in the ideal triangular lattices [20], but also if they are randomly modified by adding or removing some links, provided that the resulting graph density is not too far from that characteristic to the regular grid [7].

However, the density of classical random graph has a decisive impact on how the transition between balanced and imbalanced states proceeds. Our results show that above a certain minimal density, a phase transition of

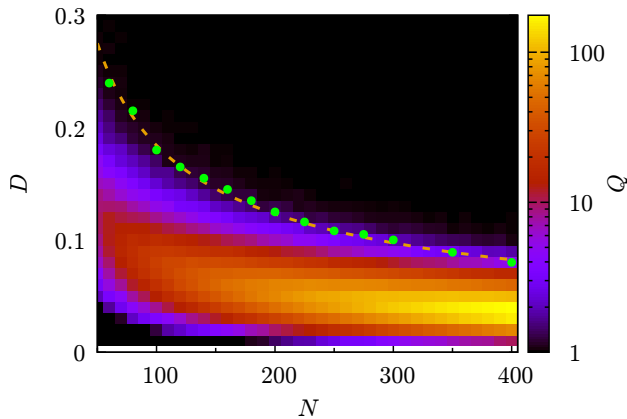


FIG. 6: The number of clusters of interacting triads, Q , as a function of the system size N and graph density D . Green dots represent the values of minimal density D_{\min} allowing the phase transition (see Figure 4).

the first kind is observed, with the critical temperature dependent on the system size. It is possible, nonetheless, to define a reduced critical temperature that is size-independent and scales with size as $T_c^* \propto D^{1.719(6)}$. Above the minimal density required for the phase transition, a gradual and smooth crossover between balanced and imbalanced states occurs. It turns out that the minimal density mentioned above also varies with the size of the system, changing exponentially as $D_{\min} \propto N^{-0.58(1)}$. The presence of the phase transition is directly related to the number of clusters of triads that may interact (at least indirectly) during time evolution: we show that it is possible only when the system consists of a large enough number of triads organized into just one or a small number of such clusters.

ACKNOWLEDGMENTS

The authors are grateful to Krzysztof Kułakowski for fruitful discussion and critical reading of the manuscript.

-
- [1] F. Harary, “On the notion of balance of a signed graph,” *Michigan Mathematical Journal* **2**, 143–146 (1953); D. Cartwright and F. Harary, “Structural balance: A generalization of Heider’s theory,” *Psychological Review* **63**, 277–293 (1956); F. Harary, “On the measurement of structural balance,” *Behavioral Science* **4**, 316–323 (1959); J. A. Davis, “Clustering and structural balance in graphs,” *Human Relations* **20**, 181–187 (1967); F. Harary, R. Z. Norman, and D. Cartwright, *Structural Models: An Introduction to the Theory of Directed Graphs*, 3rd ed. (John Wiley and Sons, New York, 1965).
- [2] F. Heider, “Attitudes and cognitive organization,” *The Journal of Psychology* **21**, 107–112 (1946).
- [3] L. Festinger, *A Theory of Cognitive Dissonance* (Stanford University Press, Stanford, 1957); “Cognitive dissonance,” *Scientific American* **207**, 93–102 (1962).
- [4] A. M. Belaza, K. Hoefman, J. Ryckebusch, A. Bramson, M. van den Heuvel, and K. Schoors, “Statistical physics of balance theory,” *Plos One* **12**, e0183696 (2017).
- [5] K. Malarz, M. Wołoszyn, and K. Kułakowski, “Towards the Heider balance with a cellular automaton,” *Physica D* **411**, 132556 (2020).
- [6] M. J. Krawczyk, K. Kułakowski, and Z. Burda, “Towards the Heider balance: Cellular automaton with a global neighborhood,” *Physical Review E* **104**, 024307 (2021).
- [7] M. Wołoszyn and K. Malarz, “Thermal properties of structurally balanced systems on diluted and densified triangulations,” *Physical Review E* **105**, 024301 (2022).
- [8] M. J. Krawczyk, M. del Castillo-Mussot, E. Hernandez-Ramirez, G. G. Naumis, and K. Kułakowski, “Heider balance, asymmetric ties, and gender segregation,” *Physica A* **439**, 66–74 (2015).
- [9] P. Gawroński, M. J. Krawczyk, and K. Kułakowski, “Emerging communities in networks—A flow of ties,” *Acta Physica Polonica B* **46**, 911–921 (2015).
- [10] P. Gawroński and K. Kułakowski, “A numerical trip to social psychology: Long-living states of cognitive dissonance,” *Lecture Notes in Computer Science* **4490**, 43–50 (2007).
- [11] P. Gawroński, P. Groniek, and K. Kułakowski, “The Heider balance and social distance,” *Acta Physica Polonica B* **36**, 2549–2558 (2005).
- [12] S. A. Marvel, J. Kleinberg, R. D. Kleinberg, and S. H. Strogatz, “Continuous-time model of structural balance,” *Proceedings of the National Academy of Sciences* **108**, 1771–1776 (2011).
- [13] K. Kułakowski, P. Gawroński, and P. Groniek, “The Heider balance: A continuous approach,” *International Journal of Modern Physics C* **16**, 707–716 (2005).
- [14] K. Kułakowski, M. Stojkow, and D. Żuchowska-Skiba, “Heider balance, prejudices and size effect,” *The Journal of Mathematical Sociology* **44**, 129–137 (2020).
- [15] T. Antal, P. L. Krapivsky, and S. Redner, “Dynamics of social balance on networks,” *Physical Review E* **72**, 036121 (2005).
- [16] K. Kułakowski, “A note on temperature without energy—A social example,” (2008), arXiv:0807.0711 [physics.soc-ph].
- [17] C. Michael, “Fast heat-bath algorithm for the Ising model,” *Physical Review B* **33**, 7861–7862 (1986).
- [18] D. Loison, C. L. Qin, K. D. Schotte, and X. F. Jin, “Canonical local algorithms for spin systems: Heat bath and Hastings’s methods,” *The European Physical Journal B* **41**, 395–412 (2004).
- [19] K. Malarz and K. Kułakowski, “Heider balance of a chain of actors as dependent on the interaction range and a thermal noise,” *Physica A* **567**, 125640 (2021).
- [20] K. Malarz and M. Wołoszyn, “Expulsion from structurally balanced paradise,” *Chaos* **30**, 121103 (2020).
- [21] F. Rabbani, A. H. Shirazi, and G. R. Jafari, “Mean-field solution of structural balance dynamics in nonzero

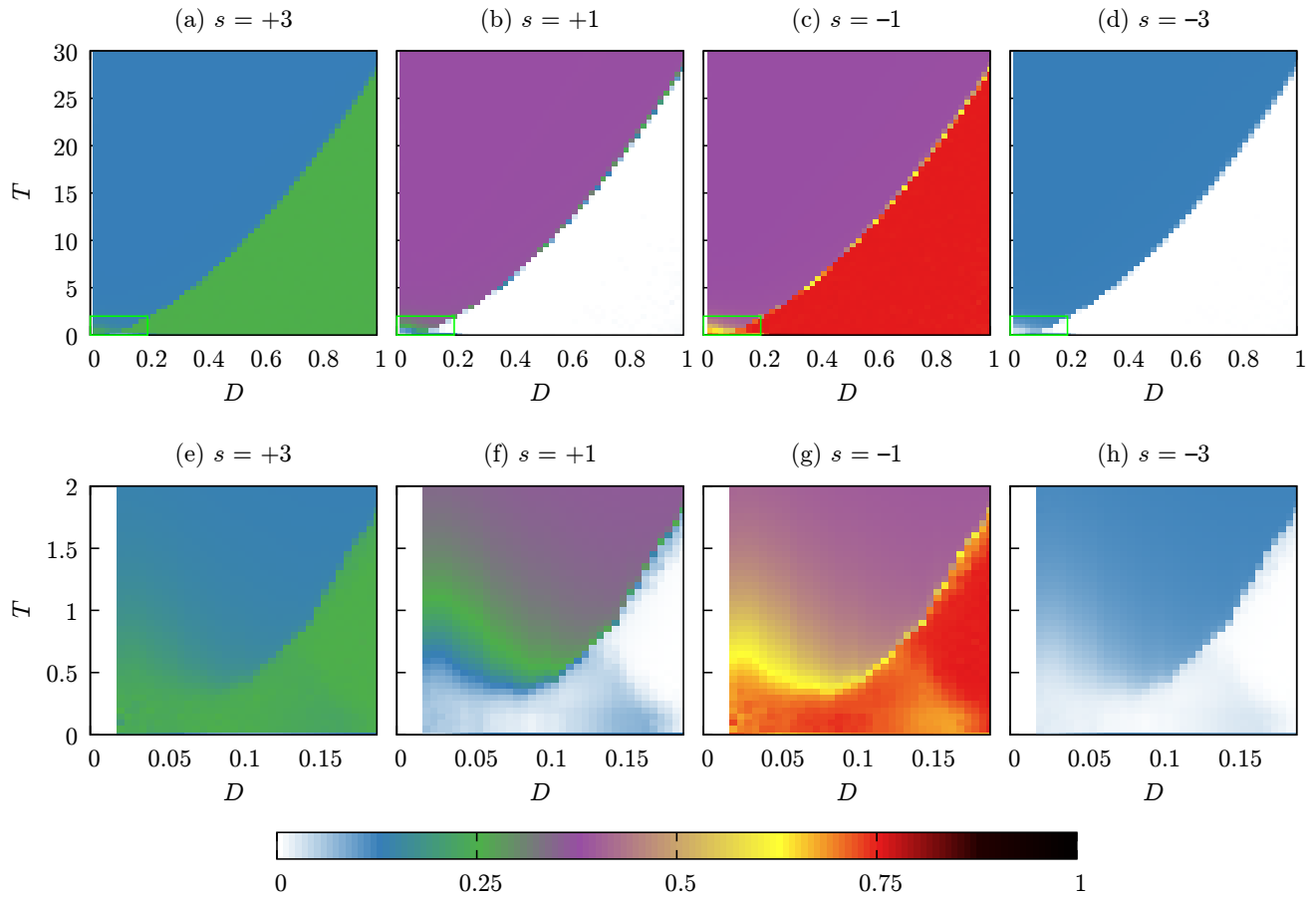


FIG. 7: Dependence of the fraction of balanced [(a, e) $s = +3$ and (c, g) $s = -1$] and imbalanced [(b, f) $s = +1$ and (d, h) $s = -3$] triads on density D and temperature T calculated for $N = 200$. (e–h) Detailed view for the range of low D and low T indicated with green rectangles in (a–d).

- temperature,” *Physical Review E* **99**, 062302 (2019).
- [22] R. Shojaei, P. Manshour, and A. Montakhab, “Phase transition in a network model of social balance with Glauber dynamics,” *Physical Review E* **100**, 022303 (2019).
- [23] K. Malarz and K. Kułakowski, “Comment on ‘Phase transition in a network model of social balance with Glauber dynamics’,” *Physical Review E* **103**, 066301 (2021).
- [24] P. Manshour and A. Montakhab, “Reply to ‘Comment on ‘Phase transition in a network model of social balance with Glauber dynamics’,’” *Physical Review E* **103**, 066302 (2021).
- [25] R. Masoumi, F. Oloomi, A. Kargaran, A. Hosseiny, and G. R. Jafari, “Mean-field solution for critical behavior of signed networks in competitive balance theory,” *Physical Review E* **103**, 052301 (2021).
- [26] K. Malarz and J. A. Hołyst, “Mean-field approximation for structural balance dynamics in heat-bath,” (2019), [arXiv:1911.13048](https://arxiv.org/abs/1911.13048) [physics.soc-ph].
- [27] A. Kargaran and G. R. Jafari, “Heider and coevolutionary balance: From discrete to continuous phase transition,” *Physical Review E* **103**, 052302 (2021).
- [28] P. Erdős and A. Rényi, “On random graphs. I,” *Publicationes Mathematicae* **6**, 290–297 (1959).
- [29] P. Erdős and A. Rényi, “On the evolution of random graphs,” *Publications of the Mathematical Institute of the Hungarian Academy of Sciences* **5**, 17–61 (1960).
- [30] B. Bollobás, *Random Graphs*, 2nd ed., Cambridge Studies in Advanced Mathematics (Cambridge University Press, 2001).
- [31] A. Frieze and M. Karoński, *Introduction to Random Graphs* (Cambridge University Press, 2015).
- [32] D. P. Landau and K. Binder, *A Guide to Monte Carlo Simulations in Statistical Physics*, 3rd ed. (Cambridge University Press, 2009).
- [33] E. N. Gilbert, “Random graphs,” *The Annals of Mathematical Statistics* **30**, 1141–1144 (1959).
- [34] K. Malarz and K. Kułakowski, “Matrix representation of evolving networks,” *Acta Physica Polonica B* **36**, 2523–2536 (2005).
- [35] M. J. Krawczyk, S. Kaluzny, and K. Kułakowski, “A small chance of paradise—Equivalence of balanced states,” *EPL (Europhysics Letters)* **118**, 58005 (2017).
- [36] M. S. S. Challa, D. P. Landau, and K. Binder, “Finite-size effects at temperature-driven first-order transitions,” *Physical Review B* **34**, 1841–1852 (1986).
- [37] M. Acharyya, “Nonequilibrium phase transition in the kinetic Ising model: Existence of a tricritical point and stochastic resonance,” *Physical Review E* **59**, 218–221

- (1999).
- [38] K. Binder, “Applications of Monte Carlo methods to statistical physics,” *Reports on Progress in Physics* **60**, 487–559 (1997).
- [39] J. Hoshen and R. Kopelman, “Percolation and cluster distribution. 1. Cluster multiple labeling technique and critical concentration algorithm,” *Physical Review B* **14**, 3438–3445 (1976); S. Frijters, T. Krüger, and J. Harting, “Parallelised Hoshen–Kopelman algorithm for lattice-Boltzmann simulations,” *Computer Physics Communications* **189**, 92–98 (2015); M. Kotwica, P. Groniek, and K. Malarz, “Efficient space virtualisation for Hoshen–Kopelman algorithm,” *International Journal of Modern Physics C* **30**, 1950055 (2019).